HYDRODYNAMICS OF QUARK-GLUON PLASMAS*

BY J.-P. BLAIZOT

Service de Physique Théorique, CEA-Saclay**

(Received October 21, 1986)

This paper reviews some aspects of the hydrodynamics of quark-gluon plasmas. Various stages of ultra-relativistic heavy ion collisions are described. Several estimates of the maximum energy density expected to be achieved in these collisions are compared. Discontinuities which may be induced in the hydrodynamic flow by a phase transition are described and a convenient numerical method designed to deal with such discontinuous flows is briefly presented. Finally, the correlations between particle transverse momenta and multiplicities are analyzed and one discusses to which extent these correlations could signal the occurrence of a phase transition in heavy ion collisions.

PACS numbers: 12.38.Mh

1. Introduction

One of the main goals of the study of ultra-relativistic heavy ion collisions is to understand the behaviour of extended hadronic systems under extreme conditions of temperature or baryon density. In particular one hopes, if the energy densities achieved in the collisions are high enough, to induce the so-called deconfinement transition leading to the formation of a quark–gluon plasma (for a general review of the field see [1]).

But what is a quark-gluon plasma?... One must recognize that our theoretical knowledge of this new state of matter predicted by quantum chromodynamics is still very primitive. The qualitative picture which emerges from lattice gauge calculations is summarized in Fig. 1 which displays the energy density of baryonless matter as a function of the temperature. The energy density (in units of T^4) exhibits a characteristic increase within a narrow temperature interval centered around T_c, and quickly reaches a saturating value above T_c. In all calculations done so far, it appears that the value of thee nergy density at high temperature is compatible with the Stefan-Boltzmann law for a gas of non interacting quarks and gluons [2]. This could be naively expected on the basis of asymptotic freedom and it provides the simplest picture one may have of a quark–gluon plasma, namely that of a gas

* Presented at the XXVI Cracow School of Theoretical Physics, Zakopane, Poland, June 1–13, 1986.

** Address: Service de Physique Théorique, CEA-Saclay, 91191 Gif-sur-Yvette Cedex, France.

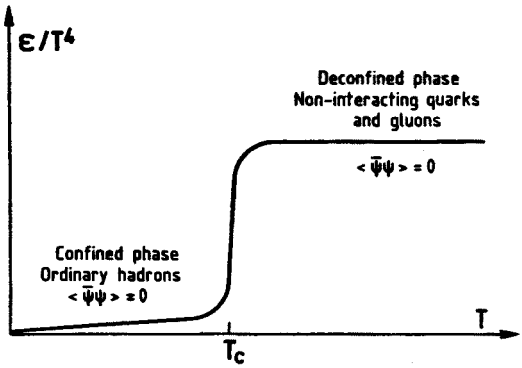

Fig. 1. Schematic representation of the energy density of baryonless hadronic matter as a function of the temperature

of weakly interacting particles. However, it is worth keeping in mind that this simple picture may turn out to be too naive and that the elementary modes of excitations of the plasma may be more complicated objects than free quarks and gluons (recent calculations seem to indicate that the high temperature phase of QCD may contain chromomagnetic monopoles [3]). Furthermore ambiguities remain regarding the physical significance of the rapid variation of the energy density at T_c. For pure SU(3) gauge theories, it has been established that this phenomenon is to be associated with a first order deconfinement transition [4]. When dynamical quarks are taken into account, the calculations become much more complicated and correspondingly the conclusions are less definite. This is even more so at finite baryon density [5]. Is there a phase transition at $T = T_c$? If yes, is this transition first or second order? Is the restoration of chiral symmetry closely related to the deconfinement transition, as suggested by some calculations?... Answers to these questions, among many others, do require more theoretical work. But in spite of all those question-marks, it is now commonly accepted that a quark–gluon plasma may be produced whenever the energy density exceeds a critical value of the order of a few GeV per fm^3 (the precise value of this number is still uncertain, as is the value of the transition temperature, T_c, believed to be of the order of 200 MeV).

The only laboratory systems in which one can possibly produce such high energy densities are colliding heavy ions. We shall see explicitly that the energy density achieved in ultra-relativistic nucleus–nucleus collisions is indeed expected to grow significantly with the size of the nuclei involved. Unfortunately, colliding heavy ions are rather complicated dynamical systems. They are at low energies and extra complications come in at ultra-relativistic energies: particle production mechanisms are still poorly understood. Furthermore, not only are we interested in producing hadronic systems with a large energy density, but we want those systems to live long enough to exhibit interesting and recognizable physical properties. Ideally, we would like to produce the plasma at rest and study its thermodynamical properties. Clearly, this ideal situation can hardly be achieved in nucleus–nucleus collisions which are rather transient phenomena.

In this context, the task of finding unambiguous signatures of the effects of the

plasma — or rather of what we think a plasma is — on an a-priori complicated dynamics may appear at first as an hopeless task. However, the importance of the issue is certainly worth some efforts. Besides, the situation is not quite as dark as these introductory lines may tend to suggest. There has been considerable progress over the last few years in our understanding of the physics which may be expected in ultra-relativistic nucleus–nucleus collisions. Furthermore, the forthcoming experiments at CERN and BNL will soon provide invaluable information and transform what has been up to now perhaps a rather speculative domain into a more sound field of physics.

These lecture notes are devoted to the description of a fairly idealized situation, that of a perfectly central collision at an extremely high energy. Such a model study may be somewhat unrealistic as far as comparison with experiment is concerned. Its main virtue is to help developing our intuition and to provide a rather clear conceptual framework within which many interesting physical questions may be formulated.

Much of the results presented here were obtained in collaboration with J. Y. Ollitrault [22, 19]. Very similar investigations were carried out independently by V. Ruuskanen and his collaborators. There will be therefore some overlap between this and Ruuskanen's lecture [20], and also to a less extent with that of Friman [28].

2. *Space-time description of collisions and hydrodynamics*

In order to make progress in the description of nucleus–nucleus collisions simplifying assumptions concerning the dynamics are necessary. Also, it is helpful to simplify as much as possible the geometry of the systems one wishes to study. An obvious simplification occurs if one restricts oneself to central collisions of identical nuclei, since then one may take advantage of the cylindrical symmetry. At high energies, one expects nuclei to go through each other leaving between them a "central region" which contains very few baryons (Fig. 2). The evolution of this central region is simpler to analyze than the fragmentation regions which contain all the baryons. A further simplification comes from assuming that the particle production process in the central region is invariant under Lorentz boosts along the longitudinal direction, as predicted by most particle production models. Cylindrical symmetry and longitudinal boost invariance reduce our problem effectively to a 1+1 dimensional problem.

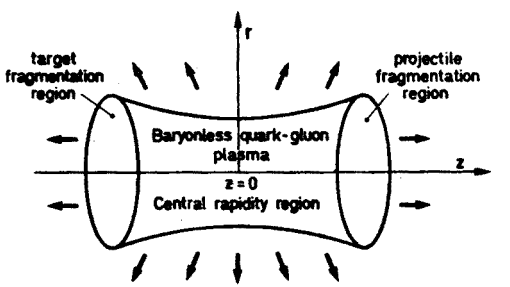

Fig. 2. Representation of an idealized central collision between two identical nuclei. The baryons populate the Lorentz contracted fragmentation regions. The central rapidity region is baryon free

A further major step in arriving at a simple picture is to assume that the quarks and the gluons produced in the initial stages of the collision quickly thermalize. If this is so, the evolution of the quark–gluon plasma, once formed, may be described by hydrodynamics. There are two basic ingredients in hydrodynamics. One is a statement of local conservation of energy and momentum, which can be expressed in the form:

$$\partial_\mu T^{\mu\nu} = 0. \tag{2.1}$$

This equation is much more general, of course, than hydrodynamics. Any local field theory would lead to Eq. (2.1). Specific aspects of hydrodynamics enter in the prescription of the form of the energy–momentum tensor $T^{\mu\nu}$. If one ignores dissipative processes as is done in most calculations, one finds [6]:

$$T^{\mu\nu} = (\varepsilon + P)u^\mu u^\nu - Pg^{\mu\nu}, \tag{2.2}$$

where $g^{\mu\nu}$ is the metric tensor, u^μ the fluid four-velocity, ε the energy density and P the pressure. The pressure and the energy density are related by an equation of state:

$$P = P(\varepsilon). \tag{2.3}$$

The equations (2.1–2.3) certainly constitute the simplest set of dynamical equations capable of describing the evolution of the baryonless plasma. Also, they directly incorporate our available microscopic information about plasma properties through the equation of state. Finally, since they deal mostly with basic conservation laws, they should provide reasonable orientation for average properties.

The most important assumption done in writing the equations (2.2–3) concerns the thermalization. Whether this thermalization does occur, and over a sufficiently short period of time for the whole picture to make sense is still an unproved conjecture. One can give however some plausibility arguments based on mean free path estimates. The mean free path is given by:

$$\lambda = 1/\sigma n, \tag{2.4}$$

where σ is the quark or gluon cross-section in the plasma and n the number density of the plasma. If ones assumes thermalization at a temperature T, one can calculate the number of quanta to be:

$$n = \frac{\zeta(3)}{\pi^2}(\nu_B + \tfrac{3}{4}\nu_F)T^3, \tag{2.5}$$

where ν_B and ν_F are the numbers of boson and fermion species in the plasma, respectively. In a baryonless plasma made of u and d quarks, in addition to gluons, one finds $n \sim 4.14\,T^3$. The average cross-section for a gluon propagating through the plasma may be estimated to be of the order of 14 mb. This is obtained as follows. The additive quark model gives the quark-hadron cross-section as about a third of the hadron-hadron cross-section, typically of the order of 40 mb. The quark-quark cross-section is itself a third of the quark-

-hadron cross-section, that is about 4.5 mb. The color algebra implies the following ratios between gluon–gluon, gluon–quark and quark–quark cross-sections:

$$\sigma_{gg} = \tfrac{9}{4}\,\sigma_{gq} = (\tfrac{9}{4})^2 \sigma_{qq}. \tag{2.6}$$

Averaging over the various species present in the plasma using the equation (2.5) one finally gets the estimate mentioned above. For a plasma of u and d quarks at a temperature $T \sim 200$ MeV one finds $n \sim 4$ fm^{-3}, $\lambda \sim 0.2$ fm. Thus the mean free path is small compared to a typical size of the system, e.g. $2R \sim 15$ fm for big nuclei.

It is convenient to describe the longitudinal evolution of the system in a space-time diagram, such as the one displayed in Fig. 3. It is also useful to introduce special coordinate, referred to as the space-time proper time and rapidity, respectively:

$$\tau = \sqrt{t^2 - z^2}, \qquad \eta = \tfrac{1}{2} \ln \frac{t+z}{t-z}, \tag{2.7}$$

in terms of which one has:

$$t = \tau \cosh \eta, \qquad z = \tau \sinh \eta. \tag{2.8}$$

In this space-time diagram, the various stages of the collision are bordered by hyperbolae of constant proper time τ, as a result of the longitudinal boost invariance (physical quantities such as the energy density, the pressure, are independent of η). Let us now describe briefly these various stages.

For negative times, the two ions are moving towards each other at a speed close to that of light, and suffer a Lorentz contraction which reduces their apparent longitudinal size to $2R/\gamma$, where $\gamma = 1/\sqrt{1-v^2}$ and R is the radius of the ions. Strictly, this Lorentz contraction does not apply to the small momentum components of the nuclear wavefunctions (defined in the center of mass frame), but we shall ignore these subtleties here [7]. The nuclei

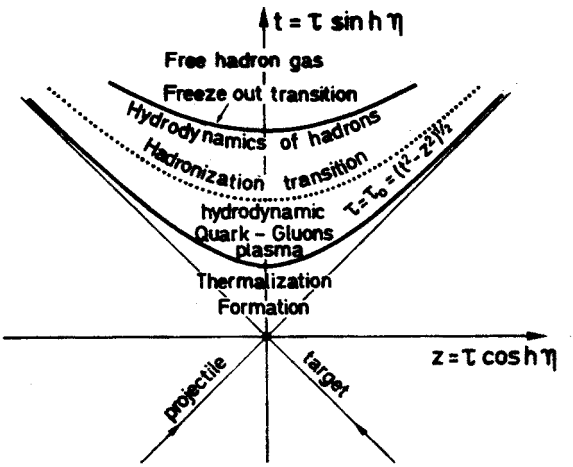

Fig. 3. Space-time diagram representing various stages of a central collision. Thesevar ious stages are separated by hyperbolae of constant proper time, as implied by the longitudinal boost invariance

collide at $z = t = 0$, and a lot of quanta get produced. The detailed mechanisms by which these quanta materialize as well identified particles are still poorly understood. But, as we already mentioned, it is generally assumed that the particle production is invariant under longitudinal boosts, namely that the initial distribution of quanta is independent of the space time rapidity η and depends only on some initial proper time τ_0 [8]. Thus in the space-time diagram of Fig. 3, the particles are created on an hyperbola labelled by τ_0. A particle which appears on this hyperbola at the space-time point (z, t) has there a velocity equal to z/t. The assumption of thermalization implies that (shortly?) after formation, the distribution of quanta is that of local thermal equilibrium:

$$n(r, p, t) = \frac{1}{\exp(\varepsilon_p/T(r, t)) \mp 1}, \quad \varepsilon_p = \sqrt{p^2 + m^2}, \tag{2.9}$$

where $T(r, t)$ is the local temperature of the system. Let us remark that the longitudinal boost invariance implies that T depends on z and t only through the combination $t^2 - z^2$, that is the proper time τ. The estimates of the formation time as well as of the time at which the system is thermalized are fairly uncertain [9]. In order to be specific in our description of the scenario, we shall assume that after a proper time of the order of one fermi, the system has reached local thermal equilibrium (see further discussion of this point in the next section). From there on the system is described by the equations of hydrodynamics.

The hydrodynamical evolution of the system may be understood as the superposition of two collective motions [10]. The first one is the longitudinal expansion of the fluid, which because of the boost invariance reduces to a simple scaling mode. Thus for example, at a given distance from the collision axis, the longitudinal expansion causes the entropy density to drop like $1/\tau$:

$$s(\tau) = s(\tau_0)\tau_0/\tau. \tag{2.10}$$

This result reflects simply the fact that the entropy is conserved during the evolution and that the proper volume of the system increases like the proper time τ. The longitudinal expansion of the system implies a rapid cooling of the plasma. Superimposed to this longitudinal expansion is the transverse motion which begins with the inwards propagation of a rarefaction wave. If no phase transition takes place in the system the rarefaction wave will reach the collision axis in a time $R/c_s = R\sqrt{3} \sim 12$ fm for a large nucleus (we have used the fact that the speed of sound in an ultrarelativistic medium is $c/\sqrt{3}$). This is a fairly long time scale compared to the time scale of the longitudinal expansion. Note for example that in a time of order 12 fm the central temperature drops by some 40% due to the longitudinal cooling alone (this is obtained from (2.10) which implies that temperature and time are related by: $T^3\tau \sim T_0^3\tau_0$, and τ_0 is taken to be 1 fm). Thus the overall hydrodynamics is by far dominated by the longitudinal expansion. However the interesting physics is contained in the transverse motion. This is because the transverse motion may be quite modified by the occurrence of a phase transition in the fluid as it cools down. In particular instabilities may develop in the transverse hydrodynamic flow [10, 11], and this strongly affects the final distribution of particles.

As the plasma cools down, it eventually reaches the critical temperature at which it may hadronize. In the framework of the hydrodynamic description, this hadronization is treated as a phase transition (the reverse of the deconfinement transition). As we already mentioned, this phase transition may have a strong influence on the transverse flow. When the hadronization is over, the system, mostly composed of pions, is still strongly interacting and its evolution described by hydrodynamics until the hadron mean-free-path becomes comparable to the size of the system. This is the so-called freeze-out transition where the particles decouple. From there on, the distributions of particles evolve as free distributions. A correct description of the freeze-out transition would require a detailed kinetic calculation. In the framework of the hydrodynamical model, one usually assumes that freeze-out takes place when the temperature has dropped down to some value $T_{\text{f.o.}}$, called the freeze--out temperature [12]. This is usually taken to be of the order of the pion mass for the reason that the pion mean-free-path, which is inversely proportional to the pion density, increases rapidly as the temperature decreases below the pion mass.

3. The initial energy density in the central rapidity region

The highest energy density achieved in the collision is a useful number to know, as it largely determines the state of the matter produced initially. Of course there is some ambiguity in the very definition of this quantity, which furthermore is not so easy to measure. However it is a worthwhile exercise to go through various models of particle production and see how in each case the question may be phrased. As we proceed, some general features will emerge. We shall in particular concentrate on the A-dependence of the initial energy density.

In hydrodynamics, the initial energy density is obtained by running the evolution backwards in time. One may then define the initial energy density as being the energy density at the time τ_0 at which thermal equilibrium is first achieved. The initial energy density is then a function of the initial temperature T_0, which itself is related to the initial entropy S_0. To a good approximation, the entropy is conserved in the hydrodynamic evolution: $S_f \sim S_0$. As for the final entropy, S_f, it may be calculated from the total number of produced particles. More precisely the multiplicity per unit rapidity of the produced particles is given by:

$$\left(\frac{dN}{dy}\right)_{A-A} = \frac{1}{3.6}\frac{dS_f}{dy} = \frac{1}{3.6}\pi R_0^2 s_0 \tau_0, \tag{3.1}$$

where s_0 is the initial entropy density, i.e. the entropy density at proper time τ_0. Assuming that the multiplicity in A–A collisions scales like A, one gets from (3.1) that $s_0\tau_0$ scales like $A^{1/3}$, or, since $s_0 \sim T_0^3$:

$$T_0^3 \tau_0 \sim A^{1/3}. \tag{3.2}$$

In the absence of a detailed knowledge of the microscopic mechanisms leading to thermal equilibrium one may invoke the uncertainty principle to put constraints on allowed values

of the initial temperature T_0 or the initial proper time τ_0. A simple argument shows that quantum fluctuations can be safely ignored as long as:

$$T_0\tau_0 \gg 1. \tag{3.3}$$

Now, T_0 and τ_0 are related by the equation (3.2) which implies that the product $T_0\tau_0$ varies with τ_0 as $\tau_0^{2/3}$, that is it decreases as τ_0 goes to zero. Therefore it does not make sense to run the evolution too far backwards in time. The minimum time τ_0 and correspondingly the maximum temperature T_0 which can be tolerated are obtained when $T_0\tau_0 \sim 1$. Combining this with the formula (3.2), one finds the following relationships:

$$T_0 \sim A^{1/6}, \quad \tau_0 \sim A^{-1/6}, \quad \varepsilon_0 \sim A^{2/3}, \tag{3.4}$$

where we have used the fact that the energy density goes like T^4. The possible A dependence of τ_0 was suggested by McLerran in Ref. [1].

An estimate of the initial energy density can also be obtained using the parton model. In order to do so, let us consider a system of partons in the central rapidity region and with transverse momentum k_T. Clearly, the number of partons in that system grows like the number of nucleons, i.e. like A. On the other hand, the volume of the system goes as $A^{2/3}/k_T$, where $1/k_T$ measures the longitudinal size of the partons (note that k_T is the only energy scale in the problem). Since the energy per parton is k_T, one ends up with the following formula:

$$\varepsilon_0 \sim A^{1/3}k_T^2. \tag{3.5}$$

This formula can be compared to the estimate proposed by Bjorken, and which reads [8]:

$$\varepsilon_0 \sim A^{1/3}\frac{k_T}{\tau_0}, \tag{3.6}$$

where τ_0, the so-called formation time, is the time needed for the parton to come on their mass shell. Again, since k_T is the only energy scale available, it is not unreasonable to assume $\tau_0 \sim 1/k_T$, which makes (3.5) and (3.6) identical.

In the usual parton model, it is assumed that the average transverse momentum is fixed, typically of the order of 300 MeV. However, it is possible to argue that the average transverse momentum of the partons which significantly contribute to the energy density grows like $A^{1/6}$ [14]. To see that, let us evaluate the mean-free-path of the partons in the system, $\lambda = 1/\sigma n$. The cross-section σ may be taken of the form α/k_T^2, while the number density is easily evaluated to be $n \sim A^{1/3}k_T$. Thus:

$$\lambda \sim k_T/A^{1/3}. \tag{3.7}$$

The partons which will contribute dominantly to the energy density are those whose mean-free-path is of the order of the longitudinal size of the system, i.e. for which $\lambda \sim 1/k_T$. Partons which have a much larger mean-free-path have a large transverse momentum and thus interact weakly. Partons with small mean-free-path do interact strongly but since their

transverse momentum is small, they give little contribution to the energy. Thus the important partons have a transverse momentum which scales as $A^{1/6}$. Interestingly, the same result can be derived from more microscopic considerations based on an analysis of the Altarelli-Parisi equations which govern the evolution of the parton densities as a function of momentum [13, 14]. Let us also mention the recent estimate by Hwa and Kajantie who assume that k_T remains fixed, while the size in rapidity of the parton system which will eventually thermalize is allowed to grow with A. The scaling behaviour of the energy density they obtain is identical to Eq. (3.5).

There is still another popular family of models used to describe the initial stages of the collision, and which we shall refer to as flux tube models. In such models, one assumes that the collision is initiated by a large amount of gluon exchanges, so that a large flux tube is spanned between the two receding ions [15, 16]. The color electric field is assumed to be coherent over a transverse size taken to be typically that of a proton, forming so-called elementary tubes. Particles (quarks, antiquarks and gluons) are then produced in each of these elementary tubes by tunneling, in very much the same way as electron–positron pairs are produced in a strong electric field [17]. With reasonable assumptions, one can easily estimate how the various physical quantities scale with A in this model.

First, we note that the number of gluon exchanges producing the electric field in an elementary tube goes as $\nu \sim A^{2/3}$, that is as the number of nucleon–nucleon collisions involved in the collision of two tubes of length $A^{1/3}$. Assuming that the charge resulting from these gluon exchange builds up in a random way, and that the produced electric field is proportional to the charge, one finds:

$$E_0 \sim \sqrt{\nu} \sim A^{1/3}. \tag{3.8}$$

Note that if only the color charge carried by the valence quarks were allowed to fluctuate, one would get a different result since then the charge would grow only as $A^{1/6}$. The rate of production of massless particles is given by:

$$\frac{dN}{d^4x} \sim E_0^2. \tag{3.9}$$

This may be understood simply from dimensional analysis, noting that the electric field E_0 is the only quantity in the problem which carries a dimension. Similar dimensional analysis leads to:

$$\tau_0 \sim \frac{1}{\sqrt{E_0}} \sim A^{-1/6}, \tag{3.10}$$

where τ_0 is the time scale governing the pair production process. In order to get from the rate to the total multiplicity, one needs to integrate over a space-time domain. The elementary volume element is typically of the form area $\times\, \tau dy \times d\tau$, where area is a fixed transverse area and τdy the longitudinal extension. For a fixed rapidity interval dy the integrated volume scales therefore as τ_0^2, i.e. as $A^{-1/3}$. Thus the multiplicity of the particles produced

in one elementary tube is given by:

$$\left.\frac{dN}{dy}\right|_{\text{elem}} \sim A^{-1/3}E_0^3 \sim A^{1/3}. \tag{3.11}$$

This result is compatible with the one used earlier: since the number of elementary tubes scales like $A^{2/3}$, the total multiplicity scales like A. One can continue this analysis and show that the average transverse energy per unit rapidity goes as [18]:

$$\frac{dE_T}{dy} \sim A^{-1/3}E_0^{5/2} \sim A^{1/2}. \tag{3.12}$$

It follows that the average transverse energy per particle is given by:

$$\langle E_T \rangle = \frac{dE_T/dy}{dN/dy} \sim A^{1/6}. \tag{3.13}$$

This digression illustrates how little one really understands about the very beginning of the collision, how the particles (or in the thermodynamical language the entropy) are produced, how the energy density builds up. However fairly general statements can be made about the dependence of some important observables upon the control parameters in the problem such as for example the mass number. An important result of the foregoing discussion is that the initial energy density is expected to grow with A like $A^{2/3}$, implying that the energy density achievable in a nucleus–nucleus collision is much higher than in a proton–proton collision.

We wish to conclude this discussion of the initial conditions by indicating how in the hydrodynamic model, these could be related to observables like the multiplicity of final particles. It turns out that the relevant dimensionless parameter which governs the hydrodynamic flow for the geometry we have considered is $s_0\tau_0/s_H R_0$ where s_H is the entropy density of the hadron phase at the critical temperature, s_0 is the initial entropy density, τ_0 the time at which the hydrodynamical evolution starts and R_0 the transverse size of the system [19]. It is easily seen that this parameter is proportional to the multiplicity:

$$\frac{s_0\tau_0}{s_H R_0} = \frac{3.6}{\pi R_0^3 s_H}\frac{dN}{dy} = \frac{3.6}{\pi r_0^3 s_H}\frac{1}{A}\frac{dN}{dy}. \tag{3.14}$$

Provided τ_0/R_0 is small enough, the flow at decoupling (which governs the particle momentum distributions) depends only on the ratio $s_0\tau_0/R_0$ and not on these three parameters independently.

4. Hydrodynamics with a phase transition

As we have seen in Section 1, baryonless hadronic matter is expected to undergo a phase transition at high enough temperature. This was illustrated in Fig. 1 showing the energy density as a function of the temperature. Another way to look at this phase transi-

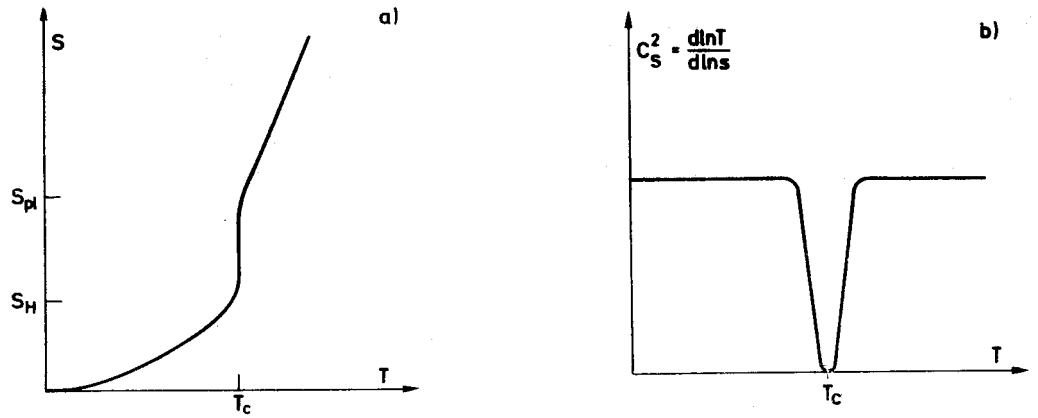

Fig. 4. (a) The entropy density as a function of temperature as may be inferred from lattice gauge calculations or from the bag model equation of state (see Ruuskanen's lecture). (b) Speed of sound squared as a function of the temperature. In the bag model equation of state, the discontinuity in the entropy density at T_c is a sharp one, and the speed of sound is a constant, equal to $1/\sqrt{3}$ at all temperatures, except at T_c where it vanishes

tion is given by Fig. 4a which shows how the entropy density varies as a function of the temperature. For the simple bag model equation of state, discussed for example in Ruuskanen's lecture, the entropy density is simply given by the formula which applies to an ideal gas of massless particles:

$$s = \nu \frac{2\pi^2}{45} T^3, \tag{4.1}$$

where ν is the number of particle species in the system. At the critical temperature, ν jumps discontinuously from a low value typical of hadronic matter ($\nu = 3$ for a massless pion gas) to a large value characteristic of a quark-gluon plasma ($\nu = 37$ for a plasma made out of gluons and u and d quarks). This rapid variation of the entropy density has a strong influence on the hydrodynamical evolution of the system. Fig. 4b shows the variation of the speed of sound c_s implied by the variation in the entropy density. Let us recall that:

$$c_s^2 = \frac{dP}{d\varepsilon} = \frac{d\ln T}{d\ln s}. \tag{4.2}$$

Away from the transition region, the speed of sound is essentially constant, and close to the ideal gas value $1/\sqrt{3}$. It decreases very rapidly as one approaches the critical temperature; in the bag model equation of state, it is exactly zero at $T = T_c$. Temperature ranges in which the speed of sound decreases as the temperature increases may lead to instabilities in the hydrodynamic flow. A simple situation where such instabilities develop is provided by the one-dimensional rarefaction wave. A typical temperature profile for such a wave is given in Fig. 5a. The arrows indicate the velocity of the flow pattern, that is the velocity of points with given temperatures. This velocity is the relativistic composition of the fluid

velocity and the sound velocity:

$$\frac{dx}{dt} = \frac{v - c_s}{1 - vc_s}. \tag{4.3}$$

In normal circumstances (as in Fig. 5a) dx/dt increases as the temperature decreases, and the wave is stable. However, if it so happens that the following condition [10] is violated

$$\frac{d}{dT}\left(\frac{sc_s}{T}\right) \geqslant 0 \tag{4.4}$$

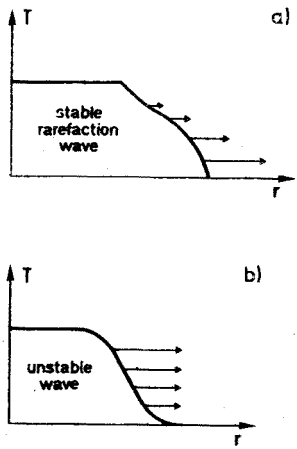

Fig. 5. (a) Temperature profile in a simple one dimensional rarefaction wave. The arrows indicate schematically the velocity of the flow pattern. (b) Same as 5a but for a speed of sound which violates the condition (4.4)

then the velocity of the pattern may decrease as the temperature decreases. In this case, illustated by Fig. 5b, the simple wave is unstable and a shock develops. Such an instability may be encountered in the transverse expansion of a quark–gluon plasma as we shall see in the next Section. A recent discussion of shock phenomena in baryonless plasma is given in Ref. [11].

In this discussion, one has implicitly assumed that the phase transition proceeds smoothly as the temperature goes through the critical temperature. This leads to a well defined scenario in which the quark–gluon plasma, as it cools down, is gradually converted into a uniform mixed phase of plasma and hadrons. More violent scenarios could be considered if one allows the plasma to supercool. These are discussed in Friman's lecture [28].

The occurrence of discontinuities in the hydrodynamic flow requires particular care in numerical calculations. We have extended [19] for this purpose a method used in non relativistic problems, and which is due to Godunov [21]. The next Section is devoted to a presentation of this method.

5. *Similarity flows and the Godunov method*

For simplicity, we shall consider here only one dimensional flows and ideal fluids. Similarity flows are particular solutions of the hydrodynamic equations in which physical quantities such as the energy density, or the fluid velocity, depend on the position x or the time t solely through the combination x/t. There are three types of similarity solutions corresponding respectively to a uniform flow, a rarefaction wave and a shock wave. A helpful representation for similarity waves is provided by $y-\zeta$ diagrams, where y denotes the fluid rapidity and ζ the flow pattern rapidity (which is equal here to the space-time rapidity η defined in (2.7)). In such a diagram, uniform flow regions are represented by horizontal lines (constant y); rarefaction waves are segments of the curves $\zeta = y \pm y_s$, and shock waves are vertical segments. The line $\zeta = y$ is a set of points where the pattern velocity is the same as the fluid velocity. Clearly such a line cannot be crossed by a shock wave or a rarefaction wave. It can only be crossed by a horizontal line corresponding to uniform flow. Examples of $y-\zeta$ diagrams are given in Figs 6 and 7. The latter corresponds to the situation to be described at length in the next Section, namely that of a mixed phase of hadrons and quark–gluon plasma being converted into a hadron gas through a rarefaction shock followed by a rarefaction wave at the Jouguet point.

A typical problem which can be solved by similarity waves is the determination of the

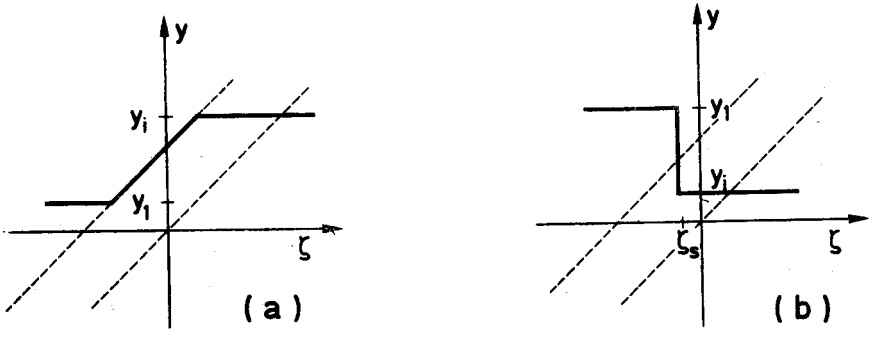

Fig. 6. y–ζ diagrams illustrating the flow patterns of a simple one-dimensional rarefaction wave (a), or a one dimensional shock wave (b), separating two regions of uniform flow

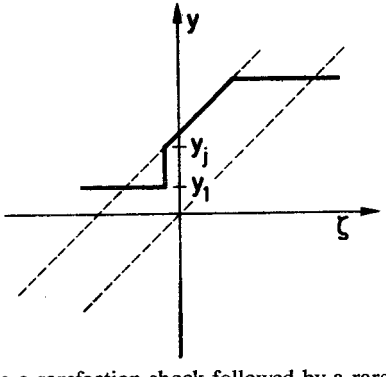

Fig. 7. y–ζ diagram representing a rarefaction shock followed by a rarefaction wave at the Jouguet point

flow pattern which connects two uniform mediums which, at time $t = 0$, occupy respectively the regions $x < 0$ and $x > 0$. Note that these initial conditions do not introduce any length scale in the problem. This is precisely the situation where one expects the flow pattern to be given by similarity waves. In general the solution to the problem consists of regions of uniform flow and rarefaction waves, separated by weak discontinuities or shock waves. This type of problem is at the heart of the Godunov method which we now describe.

As in most numerical methods for solving differential equations, we assume that space-time is dicretized into cells of area $h\tau$, where h is the step in the spatial direction, τ the step in the time direction. At the beginning of each time step, one makes all quantities characterizing the state of the fluid uniform over a cell. For example, the energy density in a cell is assumed to be constant within the cell, equal to the integral value of the true $\varepsilon(x)$ within the cell. The same is done with other quantities, such as the pressure, or the fluid velocity. During the time step τ one then solves for each pair of adjacent cells a problem analogous to the one discussed before. Note that this can be done exactly even if a shock develops in a particular cell. This is where lies the superiority of the Godunov scheme over more conventional ones. Of course the time step τ should not be taken too long to avoid that a similarity wave emanating from the boundary of a given cell reaches the other boundary. Typically τ is taken to be of the order of the spatial step. At time $t+\tau$ the evolution is frozen and the physical quantities averaged in each cell. One is then back to the situation at the beginning of the time step and the whole process can be repeated.

To test the validity of the method, we have carried out a series of numerical calculations in one dimensional situations where we could compare with the exact analytical result. Some of these calculations are presented in Refs [19, 22]. We shall just give here an illustration of the ability of the method to deal with shocks. Fig. 8 represents the flow pattern corresponding to two hadronic fluids moving into each other. The relative velocity of the two fluids has been chosen so that a double shock develops, leading to the formation of a quark–gluon plasma. This complicated flow pattern is easily handled by the Godunov method and it can furthermore be verified that the numerical and the analytical solutions are in close agreement.

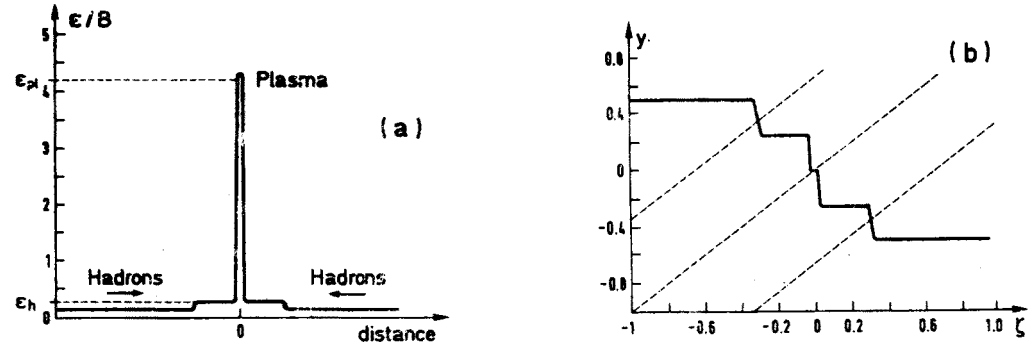

Fig. 8. Illustrative application of the Godunov method: a double shock configuration generated by two hadron fluids flowing into each other and producing a quark-gluon plasma. (a) Energy density profile. (b) y–ζ diagram

6. *Correlation between transverse momenta and multiplicities*

We shall now proceed to a discussion of some specific results of hydrodynamical calculations. The geometry of the system which we study is as discussed in Sections 1 and 2. Furthermore we assume a definite scenario for the phase transition, namely the mixed phase scenario described in Section 4.

The dominant feature of the transverse hydrodynamic flow in this scenario is the existence of a rarefaction shock converting the mixed phase into hadrons [23–25]. The effects of this shock is most easily analyzed in the one dimensional flow displayed

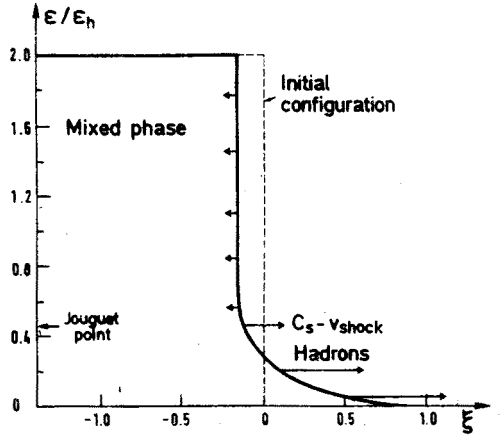

Fig. 9. Mixed phase being converted into hadrons through a rarefaction shock. This figure shows the energy density profile of a one-dimensional system as a function of $\xi = x/t$. The arrows on the profile indicate schematically the velocity of the hadrons (to the right), or of the shock (to the left)

in Fig. 9. This figure shows the energy density profile for a system prepared in a mixed phase. As time goes on, the rarefaction shock slowly moves inwards. The hadrons emerge from the shock at the speed of sound relative to the shock (Chapman-Jouguet point). It is important to observe that the velocity of the shock relative to the mixed phase decreases as the energy density, or equivalently the entropy density, in the mixed phase increases. This can be verified by an explicit calculation but is also easily understood when one knows that very little entropy is produced in the transformation of the mixed phase into hadrons (at most a few percent). The displacement of the shock into the mixed phase liberates a large amount of entropy which has to be carried away by the hadrons. Because the velocity of the hadrons is bounded when they leave the shock, there is a limit to the total amount of entropy they can carry away per unit time. This implies a slowing down of the shock with the increase of the entropy density contained in the mixed phase.

An example of temperature profile for the full three-dimensional expansion is given in Fig. 10a. This figure corresponds to a situation where a quark gluon plasma is formed initially. It can be seen that the plasma cools down fairly quickly, mostly as a result of the longitudinal expansion, and dissolves into a mixed phase of hadrons and plasma. In the

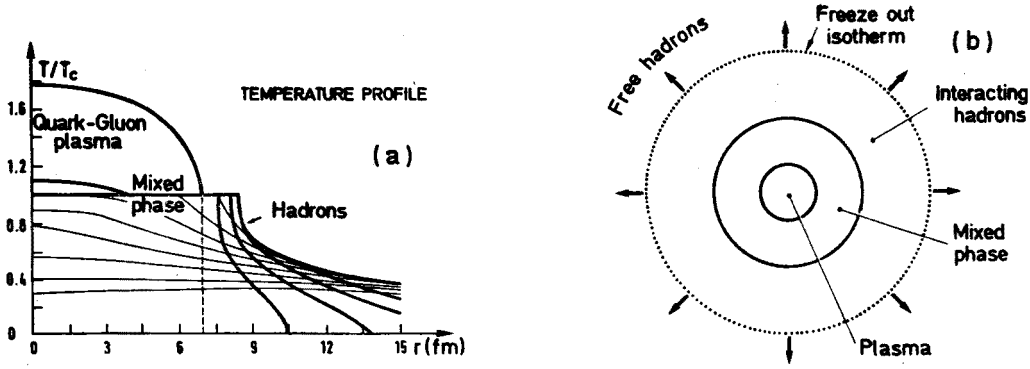

Fig. 10. (a) Temperature profile showing the transverse evolution of a quark-gluon plasma. (b) Schematic cut of the system through the plane $z = 0$ in the early stage of the evolution

mixed phase, the temperature stays constant, and a shock develops at the boundary between the mixed phase and the hadrons which surround the system (see Fig. 10b). The shock becomes weaker and weaker as time goes. This is due to the longitudinal expansion which continuously decreases the entropy of the mixed phase, making it richer and richer in hadrons. Eventually the mixed phase disappears and a hadron rarefaction wave moves inwards and reaches the collision axis. From that time on the cooling of the whole system is essentially uniform and rapid.

One of the goals of the hydrodynamical calculations is to provide a framework for the calculation of various global observables. These observables may be reconstructed from the particle distributions at freeze-out. These distribution functions have the form of local equilibrium distribution functions:

$$f(x, p) = \frac{1}{\exp\left(p^{\mu} u_{\mu} / T_{\text{f.o.}}\right) - 1}, \tag{6.1}$$

where $u_{\mu}(x)$ is the four-velocity of the fluid on the freeze-out isotherm at temperature $T_{\text{f.o.}}$. (See Section 2 for a discussion of the freeze-out transition and Ruuskanen's lecture for details concerning the calculation of the distribution functions.) A typical example of distribution is shown in Fig. 11. Three calculations are compared. In the first one (curve labelled mixed phase) it is assumed that the system is prepared in a mixed phase of hadrons and quark–gluon plasma. In the second one (curve labelled "hadrons") it is assumed that the system is initially a hadron gas, with the same entropy density (and hence a higher temperature) as in the previous case. Finally, the curve labelled "thermal" gives the distribution of a static thermal distribution at the freeze out temperature. Comparison of this distribution with the previous two shows that the acceleration of the particles due to the transverse hydrodynamical flow is not at all negligible.

The curves in Fig. 11 are very regular and much, but not all, of the physical information that one can extract from them is contained in the first moment of the distribution, that is the average transverse momentum $\langle p_{\text{T}} \rangle$. Fig. 12 is a plot of this average transverse momentum

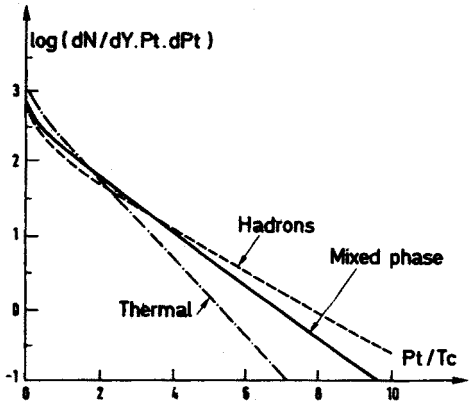

Fig. 11. Typical distribution of particle transverse momenta. The two curves labelled "mixed phase" and "hadrons" represent the results of calculations in which the system has been prepared either in a mixed phase or a pure hadronic phase, but with the same energy density in both cases. The curve labelled "thermal" refers to a calculation of the thermal distribution at the freeze-out temperature

carried away by the pions as a function of the initial entropy density. In this plot, the dashed line corresponds to the predictions obtained by ignoring the collective flows, and taking the freeze-out temperature to be the initial temperature. Let us notice that in the absence of collective flow, the particle distribution is isotropic in the laboratory frame and the average transverse momentum $\langle p_T \rangle$ is related to the mean energy per particle $\langle E \rangle$ by the equation:

$$\langle p_T \rangle = \frac{\pi}{4} \langle E \rangle. \tag{6.2}$$

Thus the curve labelled "thermal" represents the initial energy per particle as a function of the initial entropy. Using elementary thermodynamics, one can write $\langle E \rangle$ as follows:

$$\langle E \rangle = \frac{\varepsilon}{n} = \frac{\varepsilon}{\varepsilon + P} \frac{s}{n} T, \tag{6.3}$$

where s/n is the entropy per particle. For a pure hadron gas, $s/n = 3.6$, $P = \varepsilon/3$ and $\langle p_T \rangle = 2.12\, T$. As soon as one enters the mixed phase, the temperature and the pressure stay constant and a simple calculation shows that:

$$\frac{\varepsilon}{\varepsilon + P} = 1 - \tfrac{1}{4} \frac{s_H}{s}, \tag{6.4}$$

where s_H is the hadron entropy density at the critical temperature. As s goes from s_H to s_{pl}, the entropy per particle grows from 3.6 to 4.2. The maximum value of $\langle p_T \rangle$ is obtained for $s = s_{pl}$, $s/n = 4.2$, and is $3.25\, T_c$. When the entropy density of the initial state exceeds s_{pl}, the system is prepared entirely in the plasma phase, and the average transverse momentum starts to grow again, going asymptotically as $\langle p_T \rangle = 2.5$ T. Note that the slope of the

"thermal" curve in Fig. 12 is smaller for the quark–gluon plasma than for the hadron gas. This is to be attributed to the difference in the number v of degrees of freedom in the two cases ($p_T \sim T \sim v^{-1/3} s^{1/3}$). The structure observed in the dashed curve is characteristic of the rapid phase transition which takes place in the system as one increases the entropy. This behaviour has been proposed [25–27] as a possible signal for the formation of a quark–gluon plasma. However, the hydrodynamics affect this simple picture in a profound way: it may be seen in Fig. 12 (full curve) that the behaviour of the average transverse momentum as a function of entropy is deceivingly flat, exhibiting no real structure.

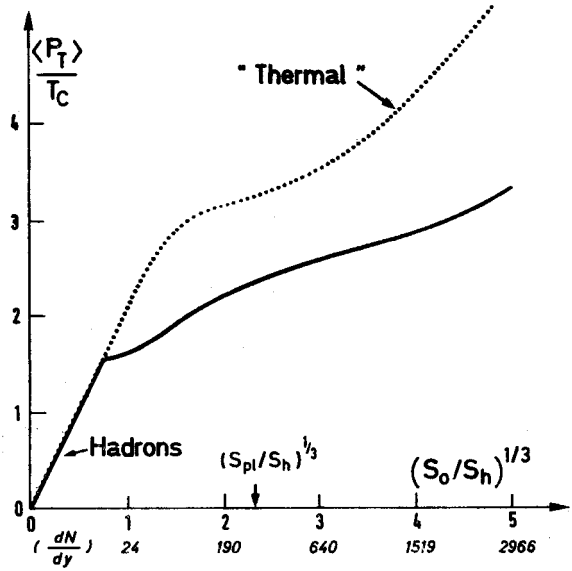

Fig. 12. Average transverse momentum as a function of the initial entropy density

The dominant agent responsible for the disappearance of the expected structure is the longitudinal cooling of the system, which largely dominates over the transverse acceleration. The transverse expansion alone would preserve (enhance) nicely the structure associated with the phase transition. This is illustrated in Fig. 13 which shows how the fluid rapidity varies at freeze-out, as a function of the initial entropy density, for a one dimensional flow. The three regimes, hadron gas, mixed phase and quark–gluon plasma are clearly exhibited. In the first regime (hadron gas), the fluid rapidity is obtained from the standard formula for a rarefaction wave:

$$y = \sqrt{3} \ln \left(\frac{s_0}{s_{f.o.}} \right)^{1/3} . \tag{6.5}$$

This formula holds as long as $s_0 \leqslant s_H$. The plateau corresponding to the mixed phase ($s_0 > s_H$) is easily understood from the discussion carried along with Fig. 9: once the nitial entropy density has reached a certain value, the rarefaction shock comes to rest

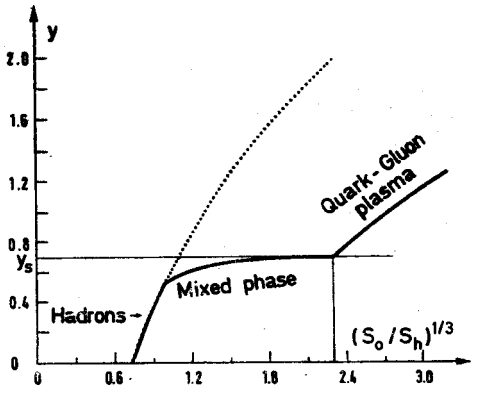

Fig. 13. Fluid rapidity as a function of the initial entropy density, for a one-dimensional flow. The dashed curve corresponds to an ideal gas of massless hadrons

and the hadrons emerge from the mixed phase at the sound rapidity and a fixed energy density ($\varepsilon = \varepsilon_H/3$). They are then further accelerated along a rarefaction wave. However due to our choice of parameters ($T_{f.o.} = 0.74\, T_c$, i.e. $s_{f.o.}/s_H = 0.4$) this extra acceleration is very small and the plateau occurs at $y \sim y_s$ where y_s is the sound rapidity. When $s_0 > s_H$, the fluid initially in the plasma is accelerated before entering the mixed phase. The corresponding increase in rapidity is given by:

$$\Delta y = \sqrt{3} \ln \left(\frac{s_0}{s_{pl}} \right)^{1/3} . \tag{6.6}$$

In order to find remnants of this behaviour in the three dimensional calculation, one has to go deeper into our analysis of the transverse momentum distributions. It is useful in this context to consider the isotherms displayed in Fig. 14. The initial part of the critical

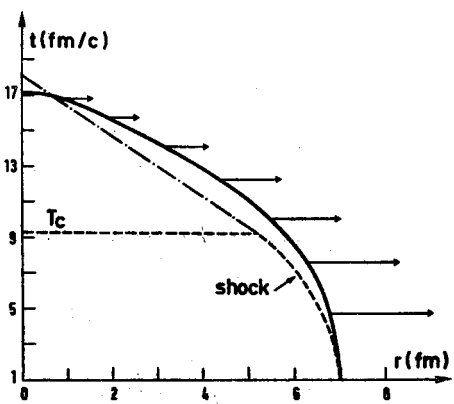

Fig. 14. Freeze-out (full line) and critical (dashed line) isotherm in the r–t plane. The magnitude of the arrows indicate schematically the velocity of the fluid on the isotherm. The dashed dotted line is the trajectory of the rarefaction front which propagates into the hadron fluid after the hadronization has been completed

isotherm coincides with the trajectory of the rarefaction shock converting the mixed phase into hadrons. For short times, the shock moves very slowly inwards, but the longitudinal expansion forces the entropy density in the mixed phase to decrease, which results in an acceleration of the shock. Eventully, the longitudinal expansion will turn all the mixed phase into hadrons before the shock reaches the collision axis. The freeze-out isotherm is also indicated in Fig. 14, together with the magnitude of the transverse velocity of the fluid on this isotherm. One sees that the particles with the largest rapidity are emitted at

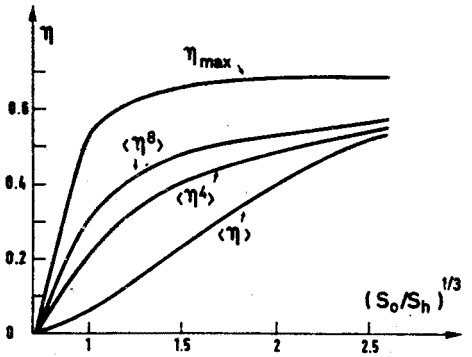

Fig. 15. Moments of the transverse rapidity distribution as a function of the initial entropy density

earlier time, and at times where the freeze-out isotherm follows a trajectory close to that of the rarefaction shock. One may therefore expect that these are the particles which have a chance to be the most sensitive to the phase transition. This is indeed confirmed by a detailed calculation reported in Fig. 15. In this figure are plotted the successive moments of the transverse rapidity distribution of the fluid. One sees that while the average rapidity does not show up any marked structure, such a structure reappears when higher moments are considered. In fact the fluid elements with the maximum rapidity are very little affected by the longitudinal expansion and the curve of η_{max} versus entropy is very much like what was obtained in the one dimensional calculation presented in Fig. 13. The role of η_{max} in the particle distribution can be seen on the asymptotic form derived in Ref. [19]:

$$\frac{dN}{dydP_T} \sim \sqrt{P_T} \exp\left(-P_T e^{-\eta_{max}}/T_{f.o.}\right). \tag{6.7}$$

Such a behaviour was found to hold for $p_T \gtrsim 5\, T_c$ [19]. By taking higher and higher moments of the momentum distribution, one gives more and more weight to the region where (6.7) holds, and in which these moments are easily seen to obey the following relation:

$$\frac{1}{n} \ln \langle P_T^n \rangle = \eta_{max} + Cste, \tag{6.8}$$

where "*Cste*" depends on n and $T_{f.o.}$ only.

7. Concluding remarks

It seems fair to say that hydrodynamical calculations are reaching the level of sophistication where they allow for the calculation of observables which can eventually be compared with experiment. We have shown that the correlations between various observables may reflect important features of the underlying equation of state. In particular, we have analyzed in detail the correlations between multiplicities and transverse momenta and discussed how they could possibly signal the occurrence of a phase transition in the evolution of the system.

However, the state of the art is still very unsatisfactory. Most of what has been done until now relies on a definite scenario for the phase transition. It is certainly the simplest, and possibly the most plausible one, but clearly more work needs to be done to get a better understanding of the dynamics of the phase transition.

Furthermore, in order to get from idealized model studies to more realistic situations, many improvements are needed. For example the freeze-out transition is crudely treated in our approach. Also, it would be desirable to get rid of the longitudinal boost invariance, to include finite baryon number and to treat the fragmentation regions. This is especially important in view of the forthcoming experiments at CERN or BNL which will deal mostly with fragmentation regions or with a baryon contaminated central region.

Finally, let us add that while hydrodynamical calculations do provide us with a useful and nice phenomenological guide to get a first orientation into the dynamics of ultra-relativistic heavy ion collisions, we should keep in mind that one still does not really understand the very beginning of the collisions during which the plasma is expected to be formed. Does the newly produced matter quickly thermalize? Are non-equilibrium phenomena playing an important role? Hopefully, the forthcoming experiments will shed some light on these important issues.

I am grateful to A. Mueller and J. Y. Ollitrault for many interesting discussions. It is a pleasure to thank our Polish friends for their warm hospitality and in particular the organizers of what has been a very enjoyable school.

REFERENCES

[1] Quark Matter 84, Proc. of the Fourth International Conference on Ultra-Relativistic Nucleus-Nucleus Collisions, ed. K. Kajantie, Lecture Notes in Physics 221, Springer-Verlag 1985.
[2] H. Satz, *Annu. Rev. Nucl. Part. Sci.* **35**, 245 (1985).
[3] J. Polonyi, in Proceedings of the International Workshop on Gross Properties of Nuclei and Nuclear Excitations XIV, ed. H. Feldmeier, Hirshegg (Austria), Jan. 1986.
[4] J. Kogut et al., *Phys. Rev. Lett.* **50**, 393 (1983); T. Celik, J. Engels, H. Satz, *Phys. Lett.* **125B**, 411 (1983).
[5] J. Kogut et al., *Nucl. Phys.* **B225** [FS9], 93 (1983); B. Berg, J. Engels, E. Kehl, B. Waltl, H. Satz, *Z. Phys.* **C31**, 167 (1986).
[6] L. D. Landau, E. M. Lifshitz, *Fluid Mechanics*, Pergamon Press, 1959.
[7] J. D. Bjorken, Lecture Notes in Physics, vol. **56**, Springer-Verlag 1976, p. 93.
[8] J. D. Bjorken, *Phys. Rev.* **D27**, 140 (1983).
[9] G. Baym, in Ref. [1], p. 39; *Phys. Lett.* **138B**, 18 (1984).

[10] G. Baym, B. L. Friman, J. P. Blaizot, M. Soyeur, W. Czyż, *Nucl. Phys.* **A407**, 541 (1983).
[11] P. Danielewicz, P. V. Ruuskanen, *Phys. Rev.* **D35**, 344 (1987).
[12] F. Cooper, G. Frye, E. Shonberg, *Phys. Rev.* **D11**, 192 (1975).
[13] A. Mueller, *Nucl. Phys.* **B268**, 427 (1986).
[14] J. P. Blaizot, A. Mueller, *Nucl. Phys.* **B289**, 861 (1987).
[15] F. Low, *Phys. Rev.* **D12**, 163 (1975); S. Nussinov, *Phys. Rev. Lett.* **34**, 1286 (1975).
[16] H. Ehtamo, J. Lindfors, L. McLerran, *Z. Phys.* **C18**, 341 (1983); T. S. Biro, H. B. Nielsen, J. Knoll, *Nucl. Phys.* **B245**, 449 (1984); A. Białas, W. Czyż, Saclay preprint SPhT/85-068.
[17] J. Schwinger, *Phys. Rev.* **82**, 664 (1951); E. Brezin, C. Itzykson, *Phys. Rev.* **D2**, 1191 (1970).
[18] A Kerman, T. Matsui, B. Svetitsky, *Phys. Rev. Lett.* **56**, 219 (1986).
[19] J. P. Blaizot, J. Y. Ollitrault, *Nucl. Phys.* **A458**, 745 (1986).
[20] P. V. Ruuskanen, *Acta Phys. Pol.* **B18**, 551 (1987).
[21] M. Holt, *Numerical Methods in Fluid Dynamics*, Springer Verlag, Berlin 1984, chapter 2.
[22] J. P. Blaizot, J. Y. Ollitrault, Proceedings of the 14th International Workshop on Gross Properties of Nuclei and Nuclear Excitations, ed. H. Feldmeier, Hirschegg (Austria), Jan. 1986.
[23] B. L. Friman, G. Baym, J. P. Blaizot, *Phys. Lett.* **132B**, 291 (1983).
[24] B. L. Friman, K. Kajantie, P. V. Ruuskanen, *Nucl. Phys.* **B266**, 468 (1986).
[25] L. Van Hove, *Z. Phys.* **C21**, 93 (1983).
[26] L. Van Hove, *Phys. Lett.* **118B**, 138 (1982).
[27] E. V. Shuryak, O. V. Zhirov, *Phys. Lett.* **89B**, 253 (1980).
[28] B. L. Friman, Lectures at the XXVI Cracow School of Theoretical Physics, Zakopane, Poland, June 1986.
[29] R. C. Hwa, K. Kajantie, *Phys. Rev. Lett.* **56**, 696 (1986).